

# Structure-Based Gene Targeting Discovery of Sphaerimicin, a Bacterial Translocase I Inhibitor\*\*

Masanori Funabashi, Satoshi Baba, Toshio Takatsu, Masaaki Kizuka, Yasuo Ohata, Masahiro Tanaka, Koichi Nonaka, Anatol P. Spork, Christian Ducho, Wei-Chen Leyla Chen, and Steven G. Van Lanen\*

Infectious and parasitic disease is estimated to be the second leading cause of death worldwide and is becoming increasingly problematic owing to the steady rise in drug-resistant pathogens.<sup>[1]</sup> The increase in resistance has also coincided with decreasing numbers of antibiotics brought to the market for the past few decades.<sup>[2]</sup> Naturally, it is paramount to global human health that new antibiotics are developed, particularly those with novel modes of action and/or unique chemical structures. Herein we present the discovery of sphaerimicin A, a sulfated hybrid polyketide–nucleoside that can be considered to fit both of these descriptors.

The peptidoglycan cell wall plays an essential role in the viability of bacteria, and as a result the inhibition of its biosynthesis has been revolutionary for treating bacterial infections.<sup>[3]</sup> Nearly all bacteria rely minimally on twelve conserved enzymes to install the cell wall, and intriguingly, the majority of these enzymes have yet to be successfully targeted by commercial antibiotics (Supporting Information, Figure S1). One of this majority is bacterial phospho-*N*-acetylmuramyl-pentapeptide translocase (translocase I, annotated as MraY), which initiates the lipid cycle of peptidoglycan biosynthesis by catalyzing the transfer of phospho-*N*-acetylmuramic acid-pentapeptide from UDP-*N*-acetylmuramic acid-pentapeptide to undecaprenyl phosphate, releasing UMP to generate undecaprenyl diphospho-*N*-acetylmuramic acid pentapeptide, or Lipid I. Within the past decade and shortly after connecting the *mraY* gene product with the translocase activity,<sup>[4]</sup> several potent natural-product inhibitors have been discovered using activity-based screens.<sup>[5]</sup> Most of the inhibitors are structurally categorized as uridine-based nucleosides wherein the canonical ribofuranose is modified at the C5' position via a C–C bond to generate a so-called high-carbon sugar nucleoside.<sup>[5]</sup> These high-carbon

sugar nucleosides are further divided into subgroups based on the core scaffold, which includes those containing the non-proteinogenic amino acid 5'-*C*-glycyluridine (GlyU) exemplified by **1–5** or those with a uridine-5'-carboxamide (CarU) core exemplified by **6–8** (Scheme 1).<sup>[6]</sup>

The biosynthetic gene clusters for **1–5** have all been identified.<sup>[7]</sup> Bioinformatic analysis uncovered a shared open reading frame (*orf*) encoding a gene product with closest sequence similarity to serine hydroxymethyltransferase (SHMT, EC 2.1.2.1; Supporting Information, Table S1), and the respective *orf* was shown to be essential for the biosynthesis of **1** and **5** upon gene inactivation.<sup>[7a,e]</sup> We have functionally assigned this SHMT-like enzyme involved in the biosynthesis of **1** as a pyridoxal-5-phosphate-dependent L-Thr:uridine-5'-aldehyde (**9**) transaldolase that generates acetaldehyde and (5'*S*,6'*S*)-GlyU (**10**; Figure 1A).<sup>[8]</sup> Rather unexpectedly, a homologous *orf* encoding the transaldolase was also uncovered within the biosynthetic gene cluster of **6** and **7** (Supporting Information, Table S1).<sup>[9]</sup> Although not biochemically confirmed, this realization suggested that CarU biosynthesis also proceeds via **9** and **10** as intermediates.

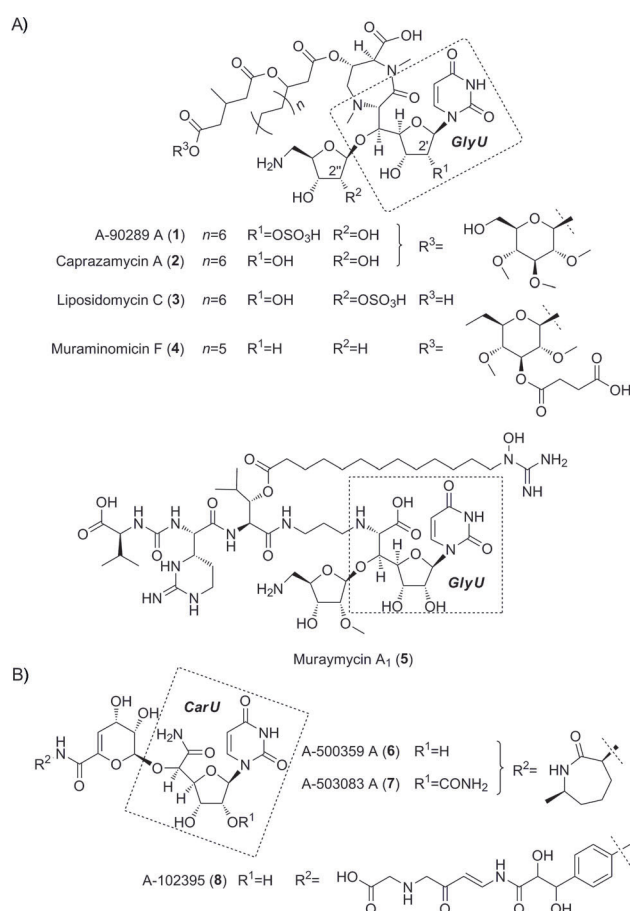
Based on the integral role of the SHMT-like transaldolase in the biosynthesis of **10**-containing inhibitors of translocase I and the likely requirement in the biosynthesis of CarU-containing inhibitors, we set out to identify similar transaldolases and thus potential novel nucleoside antibiotics from our strain collection. Sequence alignment of the transaldolases revealed blocks of conserved amino acids (Supporting Information, Figure S2) that are not observed in bona fide SHMTs (Supporting Information, Figure S3), which prompted us to develop a PCR-based strategy for screening. In contrast to mining by whole genome sequencing or activity-based screens by using a variety of fermentation conditions,

[\*] Dr. M. Funabashi, M. Kizuka, Dr. M. Tanaka  
Natural Product Research Group, Discovery Science and Technology Department, Drug Discovery and Biomedical Technology Unit, Daiichi Sankyo RD Novare Co., Ltd.  
Tokyo 134-8630 (Japan)  
Dr. T. Takatsu, Y. Ohata  
Analytical Chemistry Research Group  
Center for Pharmaceutical and Biomedical Analysis  
Daiichi Sankyo RD Novare Co., Ltd., Tokyo 134-8630 (Japan)  
Dr. S. Baba  
New Modality Research Laboratories, R&D Division  
Daiichi Sankyo Co., Ltd.  
Tokyo 140-8710 (Japan)

Dr. K. Nonaka  
Biologics Technology Research Laboratories  
R&D Division, Daiichi Sankyo Co., Ltd.  
Gunma 370-0503 (Japan)  
A. P. Spork, Prof. Dr. C. Ducho  
Department of Chemistry, University of Paderborn  
Paderborn 33098 (Germany)  
W.-C. L. Chen, Prof. Dr. S. G. Van Lanen  
Department of Pharmaceutical Sciences  
College of Pharmacy, University of Kentucky  
789 S. Limestone Street, Lexington, KY 40536 (USA)  
E-mail: svanlanen@uky.edu

[\*\*] This work was supported by NIH grant AI087849 to S.G.V.L.

Supporting information for this article is available on the WWW under <http://dx.doi.org/10.1002/anie.201305546>.



**Scheme 1.** Representative congeners for two structural groups of bacterial translocase I inhibitors that have been isolated from various actinomycetes: A,B) Nucleoside antibiotics that contain A) a 5'-C-glycyluridine (GlyU) core or B) a uridine-5'-carboxamide (CarU) core.

we considered the PCR method to be the preferred approach owing to the vast amount of strains that were targeted. Moreover, we focused on rarely-explored actinomycetes, none of which have been subjected to whole genome sequencing, as it was thought that such strains would increase the possibility of discovering compounds having novel chemical structures. Thus, degenerate primers were designed (Supporting Information, Table S2), and in contrast to results using well-characterized actinomycetes whose genomes have been sequenced and that do not produce high-carbon nucleosides, the designed primer pairs successfully and specifically amplified DNA fragments of the expected size and sequence from the genomic DNA of all the producing strains for both **10**- and CarU-containing nucleoside antibiotics (Supporting Information, Figure S4).

With the primers in hand, PCR screening was performed with a library of about 2500 strains, and DNA products of the expected size were obtained from a single strain, *Sphaerisporangium* sp. SANK 60911. Sequencing identified the amplified DNA fragment as the desired transaldolase gene (*sphJ*) having 51 % amino acid sequence identity with LipK, the characterized transaldolase involved in the biosynthesis of **1** (Supporting Information, Table S3).<sup>[8]</sup> The *sphJ* gene was

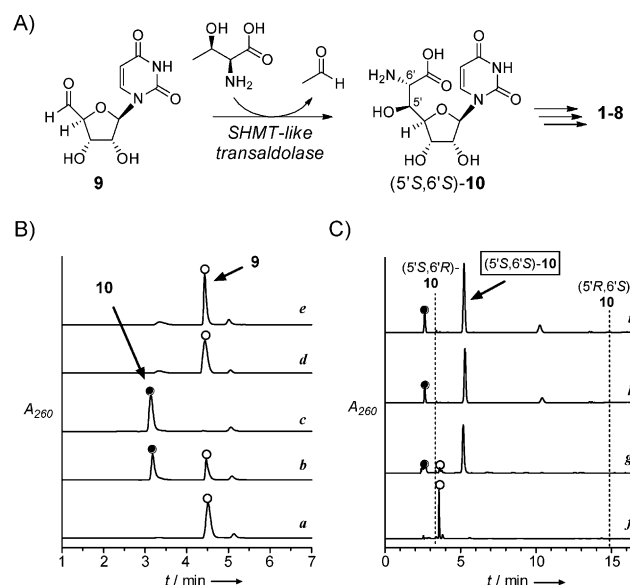


**Figure 1.** Characterization of the new family of L-Thr/9 transaldolases. A) Reaction catalyzed by the SHMT-like transaldolase enzymes, generating a shared intermediate (5'S,6'S)-**10**. B) Confirmation by HPLC of the reaction catalyzed by SphJ, including a) control reaction without L-Thr at 4 h using IMAC-purified SphJ expressed from the codon optimized gene; b) 4 h reaction; c) 12 h reaction; d) reaction at 12 h using IMAC-purified SphJ expressed from the native gene; and e) reaction at 12 h using SphJ(K248A). C) Stereochemical assignment of the SphJ product by phosgene modification, including f) control sample analyzed in (a); g) reaction components analyzed in (c); h) reaction using LipK; and i) synthetic (5'S,6'S)-**10**. Retention times are indicated for products of phosgene modification of synthetic **10** diastereomers.  $A_{260}$ : absorbance at 260 nm.

expressed in *E. coli* to confirm the expected transaldolase activity, and in contrast to the expression construct containing the native gene sequence, a protein of the expected size was apparent following IMAC when using a construct incorporating the *sphJ* gene that was optimized for expression in *E. coli* (Supporting Information, Figure S5). Using our previously developed HPLC and UV/Vis spectroscopic assays, IMAC-purified SphJ converted **9** into **10** with a specific activity of  $2.1 \times 10^{-2} \mu\text{mol min}^{-1} \text{mg}^{-1}$ , which is about 7 times lower than LipK under identical conditions (Figure 1B).<sup>[8]</sup> Continued purification of SphJ by anion exchange yielded a protein of increased specific activity ( $4.9 \times 10^{-2} \mu\text{mol min}^{-1} \text{mg}^{-1}$ ; Supporting Information, Figure S5), yet several attempts to obtain a homogenous sample by additional purification steps were unsuccessful. Therefore, a mutant protein SphJ-K248A was prepared, as it was previously established that the corresponding Lys in LipK is essential for activity;<sup>[8]</sup> as expected, SphJ(K248A) partially purified by IMAC was unable to generate **10** (Figure 1B; Supporting Information, Figure S5). Finally, HPLC analysis following phosgene modification of crude reaction mixtures in comparison to the LipK-catalyzed reaction and synthetic diastereomers of **10** revealed (5'S,6'S)-**10** as the product of SphJ (Figure 1C).<sup>[8,10]</sup>

After assigning SphJ as an L-Thr:9 transaldolase, we used *sphJ* as a probe to clone the entire genetic locus. Sequencing of four overlapping cosmids yielded 57-kb contiguous DNA consisting of 34 putative *orfs*, including *sphJ* (Supporting

Information, Figure S6 and Table S3). Eight *orfs* (*sphE-L*) were identified whose gene products have 32–51 % sequence identity to those encoded within the biosynthetic gene cluster of **1**, and one *orf* (*sphT*) for which the gene product has 48 % sequence identity to Mur29, a protein of unknown function involved in **5** biosynthesis (Supporting Information, Table S3). Furthermore, two *orfs* (*sphU* and *sphV*) encoding putative type I modular polyketide synthases and another *orf* (*sphW*) encoding a free-standing condensation domain found in nonribosomal peptide synthetases were uncovered. We chose to monitor the expression of three potentially key biosynthetic genes: *sphJ*, *sphV*, and *sphE*, a *lipL* homologue for which the gene product has been characterized as an  $\alpha$ -ketoglutarate:UMP dioxygenase in the biosynthesis of **1**,<sup>[11]</sup> to identify conditions that promote production of the corresponding metabolite. A growth condition using solid media (YMA) was found to have acceptable levels of expression of all three *orfs* (Figure 2A), and in contrast to cultures that lacked the desired expression, acetone extracts of cultures grown on YMA were shown to inhibit the activity of recombinant bacterial translocase I in vitro. HPLC analysis of these same extracts revealed four UV-active products with absorption near 260 nm that we termed sphaerimicin A–D

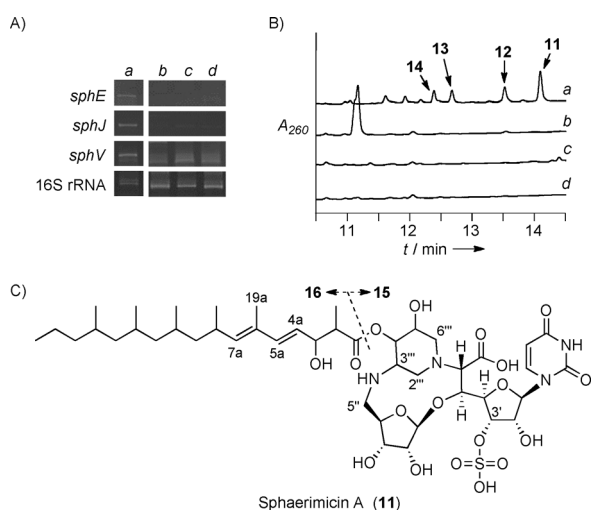


**Figure 2.** Discovery of the sphaerimicins. A) Expression analysis of the putative sphaerimicin biosynthetic genes under different cultivation conditions, including a) YMA solid media compared to b) CNZ4, c) AP-1, and d) 172F liquid media. B) Analysis of the extracts obtained from the indicated culture broths by HPLC.  $A_{260}$  = absorbance at 260 nm. C) Structure of **11** and hydrolysis products (**15** and **16**).

(**11–14**; Figure 2B). The physicochemical properties of **11–14** are summarized in the Supporting Information, Table S4.

Owing to production limitations, only **11** was purified on a large-scale for complete structural elucidation (Figure 2C). The UV absorption spectrum of **11** revealed maxima at 237 and 261 nm, which is characteristic of dienes and nucleosides, respectively. HR-ESI-MS yielded an  $[M-H]^-$  ion at  $m/z$  973.4316 (Supporting Information, Figure S7), consistent with the molecular formula of  $C_{44}H_{70}N_4O_{18}S$  (calcd. 973.4333); MS/MS gave product ions for decarboxylated-**11** ( $m/z$  929),

sulfate ( $HOSO_3^-$ ;  $m/z$  97), and uracil ( $C_4H_3N_2O_2^-$ ;  $m/z$  111) (Supporting Information, Figure S8), suggesting that **11** is an *O*-sulfated uracil-based nucleoside antibiotic with a carboxylate functionality. Similar MS/MS fragmentation ions were observed with **12–14** (Supporting Information, Figure S7). The  $^1H$ ,  $^{13}C$ , and heteronuclear 2D NMR spectra of **11** in  $[D_6]DMSO$  (Supporting Information, Table S5, Figures S9–S13) revealed 7  $CH_3$ , 8  $CH_2$ , 24  $CH$ , 4  $C=O$ , and 1  $>C=$  signals, including five olefinic protons, two anomeric carbons, several *O*- and aliphatic methines, overlapping aliphatic methylenes, and six methyl groups. This suggested that the modified nucleoside possesses a branched aliphatic side chain. Mild alkaline hydrolysis of **11** using 1N NaOH indeed gave two products (a nucleoside core **15** and acyl side chain **16**), which is consistent with a side chain linked by a standard ester bond (Figure 2C).

To simplify the structural elucidation of **11**, a thorough spectroscopic analysis was performed with **15** and **16**, and partial stereochemical assignments were facilitated in part by comparison to NMR assignments for **1–5** and various simplified, synthetic derivatives.<sup>[12]</sup> HMBC and HSQC-TOCSY analysis of **15** (Supporting Information, Figure S14–S16) revealed key  $^1H$ – $^{13}C$  and  $^1H$ – $^{15}N$  long-range correlations (Figure 3A) that were consistent with a ribosylated **10** as found in **1–5** and the fusion of the  $C5''$  amine to a dihydroxylated piperidine to give an unusual 14-membered macroheterocycle containing two bridges. The  $^{13}C$  chemical shifts of  $C5''$ ,  $2'''$ ,  $3'''$ , and  $6'''$  were also consistent with adjacency to a nitrogen and thus the structure shown for **15** (Figure 2C and 3A). The ESI-MS spectrum of **16** yielded an  $[M-H]^-$  ion at  $m/z$  365 ( $C_{23}H_{41}O_3^-$ ) that, upon MS/MS analysis, generated a product ion at  $m/z$  321 indicating **16** contains a carboxylate (Supporting Information, Figure S8). Through analysis of the  $^1H$ – $^{13}C$  HMBC and HSQC-TOCSY spectra (Supporting Information, Figures S17 and S18), the chemical structure of **16** was subsequently deduced as a branched and highly reduced, linear polyketide.

The final structural assignments were concluded based on interpretation of the NMR spectra for **11**. The connectivity of **15** and **16** was established by  $^1H$ – $^{13}C$  long-range coupling from  $H4'''$  to  $C1a$  (Figure 3B). The configuration of  $\Delta^{4a}$  was determined to be *E* based on the  $^1H$ – $^1H$  coupling constant between  $H4a$  and  $5a$  (15.5 Hz) followed by the clear NOE and ROE correlations between  $H4a$  and  $19a$  (Supporting Information, Figure S19 and S20). Likewise, NOE and ROE correlations between  $H5a$  and  $7a$  as well as  $H8a$  and  $19a$  clearly revealed that the stereochemistry of  $\Delta^{6a}$  was also *E*. Finally, three exchangeable protons were observed upon obtaining the  $^1H$  NMR spectrum of **11** in  $[D_6]DMSO$ . They were assigned to  $2'$ ,  $2''$ , and  $3a$ -hydroxy residues by the observed  $^1H$ – $^{13}C$  long-range couplings from  $OH2'$  to  $C1'$ ,  $2'$ , and  $3'$ ,  $OH2''$  to  $C1''$ ,  $2''$ , and  $3''$ , and  $OH3a$  to  $C2a$  and  $4a$  (Figure 3B). Consequently, candidate positions for *O*-sulfation were narrowed to  $C3'$ ,  $3''$ , or  $5'''$ , and thus deuterium shifts of the  $^{13}C$  signals were investigated. Among the three, only the signal assigned to  $C3'$  ( $\delta$  75.4) remained unchanged (Figure 3C). MS/MS analyses of the  $m/z$  607 and 625 product ions of **11** also supported sulfation at the hydroxy group of  $C3'$

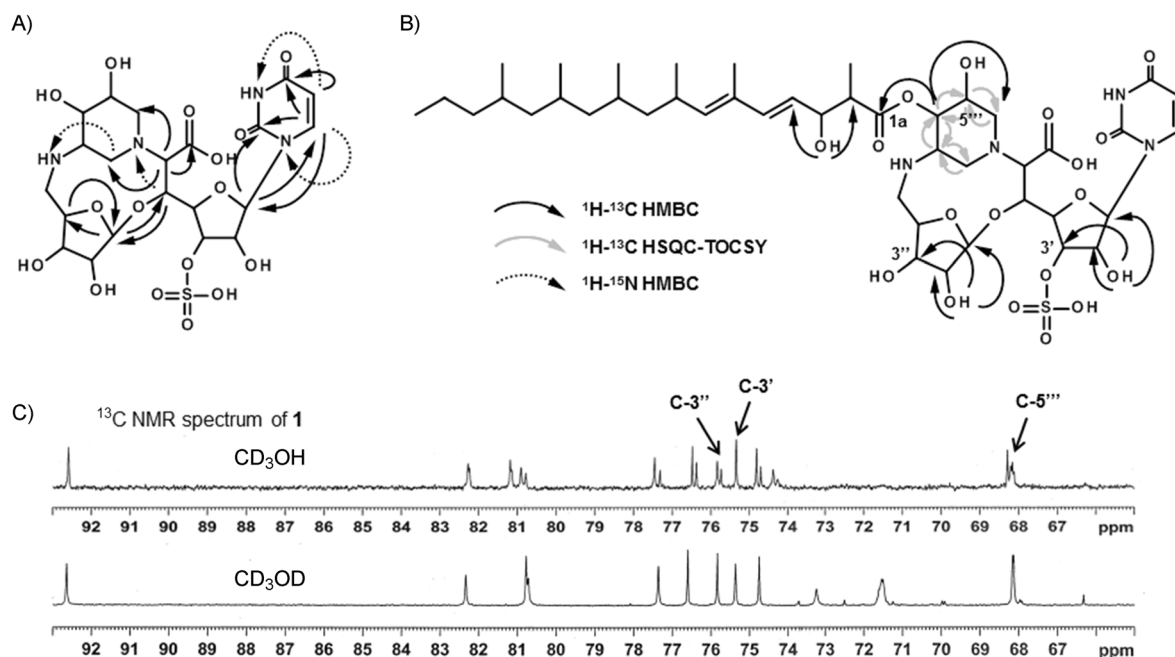


**Figure 3.** NMR analysis of spphaerimicin A. Key  $^1\text{H}$ – $^{13}\text{C}$  and  $^1\text{H}$ – $^{15}\text{N}$  long-range correlations of A) **15** and B) **11**. C) Deuterium shifts analysis of **11**.

(Supporting Information, Figure S21). In total, the final chemical structure of **11** was deduced as shown in Figure 2 C.

As expected, **11**–**14** were all potent inhibitors of bacterial translocase I with  $\text{IC}_{50}$  values between  $12\text{--}65\text{ ng mL}^{-1}$  (Figure 4), which is comparable to or better than reported values obtained with **1**–**8**. Although ineffective against Gram-negative bacteria, which is potentially a result of TolC-mediated efflux as observed with other nucleoside inhibitors of bacterial translocase I,<sup>[5]</sup> compound **11** displayed promising antibacterial activity against Gram-positive bacteria of utmost medical importance (Table 1). Moving forward, it will be of interest to investigate the role of the several unique structural features of **11** in structure–activity relationship (SAR) studies. For instance, sulfation appears to be common for the **10**-containing nucleoside antibiotics, yet the regiochemistry is different in **11** compared to **1** and **3** that contain a 2' or 2'' sulfate group, respectively. In the latter examples, this sulfation event has a pronounced negative effect on the antimicrobial activity, suggesting that desulfo-**11** may have an even better antimicrobial profile than **11**. An additional unique feature of **11** is the fused ribose and piperidine that leads to a secondary amine at C5'' of the ribosyl moiety. Prior SAR studies with simplified **2** derivatives suggested the C5'' primary amine can be replaced by

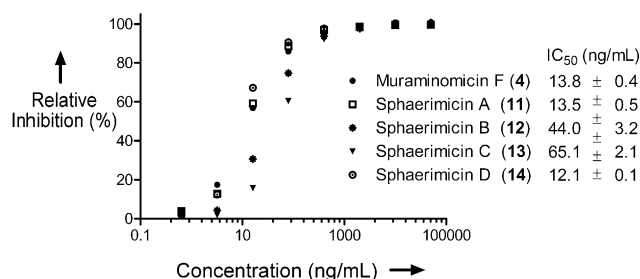


**Figure 4.** Inhibition of bacterial translocase I. For comparison, **4** was used.

**Table 1:** Antibacterial spectrum of **11**.

Test strain	Minimum inhibitory concentration ( $\mu\text{g mL}^{-1}$ )		
	Sphaerimicin A	Chloramphenicol <sup>[a]</sup>	Linezolid <sup>[a]</sup>
<i>Streptococcus pneumoniae</i> ATCC 49619 (THB)	1	2	1
<i>Streptococcus pneumoniae</i> ATCC 49619	16	2	1
<i>Streptococcus pyogenes</i> ATCC 12344	16	2	1
<i>Staphylococcus aureus</i> ATCC 6538P	4	8	2
<i>Staphylococcus aureus</i> 10925	8	16	2
<i>Staphylococcus epidermidis</i> ATCC 14990	8	4	1
<i>Enterococcus faecalis</i> ATCC 29212	2	8	2
<i>Enterococcus faecium</i> ATCC 19434	2	8	4
<i>Moraxella catarrhalis</i> ATCC 25238	4	1	4
<i>Haemophilus influenzae</i> ATCC 49247	8	1	8
<i>Haemophilus influenzae</i> Rd	32	1	8
<i>Escherichia coli</i> ATCC 47076	> 128	8	> 128
<i>Escherichia coli</i> ATCC 25922	> 128	4	> 128
<i>Klebsiella pneumoniae</i> ATCC 13883	> 128	4	> 128
<i>Enterobacter cloacae</i> ATCC 13047	> 128	8	> 128
<i>Serratia marcescens</i> ATCC 13880	> 128	8	128
<i>Proteus vulgaris</i> ATCC 13315	> 128	4	8
<i>Pseudomonas aeruginosa</i> ATCC 15692	> 128	64	> 128
<i>Stenotrophomonas maltophilia</i> ATCC 13637	> 128	4	> 128
<i>Acinetobacter baumannii</i> ATCC 19606	> 128	128	128

[a] Chloramphenicol and linezolid were used as a standard in this assay.

certain secondary amines without a significant impact on in vitro inhibitory activity,<sup>[13]</sup> and the discovery of **11** indicates the same is likely true for the overall antibacterial activity for **10**-containing nucleoside antibiotics, which was not previously tested.

In conclusion, we have discovered a novel **10**-containing nucleoside antibiotic by using a gene-guided approach, a strategy we envision can be easily applied to other strain collections or metagenomic libraries. This strategy yielded a bacterial translocase I inhibitor **11** with several unusual structural features, including a unique piperidine ring system fused to an aminoribose, a 3'-sulfate group, and a branched, highly reduced polyketide side chain. The results now pave the way to explore in greater detail how these structural features are installed and, more importantly, the application of **11** and the congeners **12–14** as new antibiotics to counteract the ever-increasing limitations of today's antibiotic arsenal.

Received: June 27, 2013

Published online: September 6, 2013

**Keywords:** actinomycetes · bacterial translocase I inhibitor · gene targeting · nucleoside antibiotics · transaldolase

- [1] World Health Organization, *The Global Burden of Disease: 2004 Update*, **2004**, p. 146.
- [2] a) G. D. Wright, *Chem. Biol.* **2012**, *19*, 3; b) M. A. Fischbach, C. T. Walsh, *Science* **2009**, *325*, 1089; c) M. A. Kohanski, D. J. Dwyer, J. J. Collins, *Nat. Rev. Microbiol.* **2010**, *8*, 423.
- [3] a) T. D. H. Bugg, C. T. Walsh, *Nat. Prod. Rep.* **1992**, *9*, 199; b) A. Bouhss, A. E. Trunkfield, T. D. Bugg, D. Mengin-Lecreulx, *FEMS Microbiol. Rev.* **2008**, *32*, 208; c) T. D. Bugg, D. Braddick, C. G. Dowson, D. I. Roper, *Trends Biotechnol.* **2011**, *29*, 163.
- [4] M. Iketa, M. Wachi, H. K. Jung, F. Ishnino, M. Matsushashi, *J. Bacteriol.* **1991**, *173*, 1021.
- [5] M. Winn, R. J. Goss, K. Kimura, T. D. Bugg, *Nat. Prod. Rep.* **2010**, *27*, 279.
- [6] a) Y. Fujita, M. Kizuka, M. Funabashi, Y. Ogawa, T. Ishikawa, K. Nonaka, T. Takatsu, *J. Antibiot.* **2011**, *64*, 495; b) M. Igarashi, Y. Takahashi, T. Shitara, H. Nakamura, H. Naganawa, T. Miyake, Y. Akamatsu, *J. Antibiot.* **2005**, *58*, 327; c) K. Kimura, Y. Ikeda, S. Kagami, M. Yoshihama, M. Ubukata, Y. Esumi, H. Osada, K. Isono, *J. Antibiot.* **1998**, *51*, 647; d) Y. Muramatsu, Y. Fujita, A. Aoyagi, M. Kizuka, T. Takatsu, S. Miyakoshi (Sankyo Co., Ltd.), Patent WO 2004046368, **2004**; e) L. A. McDonald, L. R. Barbieri, G. T. Carter, E. Lenoy, J. Lotvin, P. J. Petersen, M. M. Siegel, G. Singh, R. T. Williamson, *J. Am. Chem. Soc.* **2002**, *124*, 10260; f) Y. Muramatsu et al., *J. Antibiot.* **2003**, *56*, 243; g) Y. Muramatsu, T. Ohnuki, M. M. Ishii, M. Kizuka, R. Enokita, M. Shunichi, T. Takatsu, M. Inukai, *J. Antibiot.* **2004**, *57*, 639; h) R. Murakami, Y. Fujita, M. Kizuka, T. Kagawa, Y. Muramatsu, S. Miyakoshi, T. Takatsu, M. Inukai, *J. Antibiot.* **2007**, *60*, 690.
- [7] a) M. Funabashi, S. Baba, K. Nonaka, M. Hosobuchi, Y. Fujita, T. Shibata, S. G. Van Lanen, *ChemBioChem* **2010**, *11*, 184; b) L. Kayser, S. Siebenberg, B. Kammerer, B. Gust, *ChemBioChem* **2010**, *11*, 191; c) L. Kayser, L. Lutsch, S. Siebenberg, E. Wemakor, B. Kammerer, B. Gust, *J. Biol. Chem.* **2009**, *284*, 14987; d) X. Chi, S. Baba, N. Tibrewal, M. Funabashi, K. Nonaka, S. G. Van Lanen, *MedChemComm* **2013**, *4*, 239; e) L. Cheng, W. Chen, L. Zhai, D. Xu, T. Huang, X. Zhou, Z. Deng, *Mol. Biosyst.* **2011**, *7*, 920.
- [8] S. Barnard-Britson, X. Chi, K. Nonaka, A. P. Spork, N. Tibrewal, A. Goswami, P. Pahari, C. Ducho, J. Rohr, S. G. Van Lanen, *J. Am. Chem. Soc.* **2012**, *134*, 18514.
- [9] a) M. Funabashi, K. Nonaka, C. Yada, M. Hosobuchi, N. Masuda, T. Shibata, S. G. Van Lanen, *J. Antibiot.* **2009**, *62*, 325; b) M. Funabashi, Z. Yang, K. Nonaka, M. Hosobuchi, Y. Fujita, T. Shibata, X. Chi, S. G. Van Lanen, *Nat. Chem. Biol.* **2010**, *6*, 581.
- [10] A. P. Spork, C. Ducho, *Synlett* **2013**, 343.
- [11] Z. Yang et al., *J. Biol. Chem.* **2011**, *286*, 7885.
- [12] a) M. R. Spada, M. Ubukata, K. Isono, *Heterocycles* **1992**, *34*, 1147; b) C. Dini, P. Collette, N. Drochon, J. C. Guillot, G. Lemoine, P. Mauvais, J. Aszodi, *Bioorg. Med. Chem. Lett.* **2000**, *10*, 1839; c) S. Hirano, S. Ichikawa, A. Matsuda, *Angew. Chem.* **2005**, *117*, 1888; *Angew. Chem. Int. Ed.* **2005**, *44*, 1854; d) S. Hirano, S. Ichikawa, A. Matsuda, *Tetrahedron* **2007**, *63*, 2798; e) S. Hirano, S. Ichikawa, A. Matsuda, *J. Org. Chem.* **2008**, *73*, 569.
- [13] C. Dini, N. Drochon, S. Feteanu, J. C. Guillot, C. Peixoto, J. Aszodi, *Bioorg. Med. Chem. Lett.* **2001**, *11*, 529.